Journal of
Applied Physics

RESEARCH ARTICLE | AUGUST 15 1999

Resonance enhancement of electronic Raman scattering from nitrogen defect levels in silicon carbide

J. C. Burton; F. H. Long; I. T. Ferguson

J. Appl. Phys. 86, 2073–2077 (1999)
https://doi.org/10.1063/1.371011

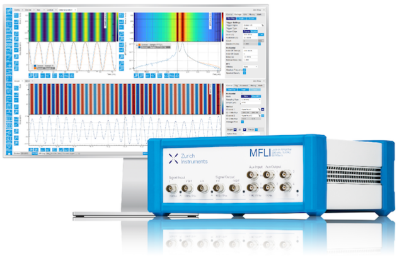

AIP Publishing

JOURNAL OF APPLIED PHYSICS VOLUME 86, NUMBER 4 15 AUGUST 1999

Resonance enhancement of electronic Raman scattering from nitrogen defect levels in silicon carbide

J. C. Burton and F. H. Long[a)]
Department of Chemistry, Rutgers University, 610 Taylor Road, Piscataway, New Jersey 08854-8087

I. T. Ferguson
EMCORE Corporation, Somerset, New Jersey 08873

(Received 25 January 1999; accepted for publication 10 May 1999)

Electronic Raman scattering from nitrogen defect levels in SiC is seen to be significantly enhanced with excitation by red (633 nm, 1.98 eV) or near-IR (785 nm, 1.58 eV) laser light at room temperature. Four nitrogen peaks are observed in 6H–SiC (380, 430, 510, and 638 cm^{-1}) and three peaks in 4H–SiC (about 400, 530, and 570 cm^{-1}). The peaks in the 4H–SiC spectrum are seen to shift to lower frequency with increasing nominal doping concentration. Raman spectra taken at low temperature in 6H–SiC reveal differences between wafers and Lely grown platelets by the appearance of several additional peaks. The origin of the resonant enhancement is the near-IR absorption band associated with the green color characteristic of *n*-type SiC. These results demonstrate that the laser wavelength is a key parameter in the characterization of SiC by Raman scattering. © *1999 American Institute of Physics.* [S0021-8979(99)03016-9]

INTRODUCTION

Recent research in the field of high-power and high-temperature electronics has focused on silicon carbide (SiC) as an important material for a wide variety of applications. SiC exhibits polytypism. There are in excess of 250 polytypes of SiC, which have the same chemical composition, but different crystallographic structures, band gaps, electron mobilities, and other physical properties.[1] Technologically, the most important polytypes are 4H– and 6H–SiC, which both have C_{6v} crystallographic symmetry and only differ significantly in the stacking along the principal crystal axis. It is only recently that high-quality wafers of both 4H– and 6H–SiC have been grown.[2,3] 4H–SiC has been subject to significant attention due to its excellent thermal properties and high electron mobility.

The one-phonon Raman spectrum of SiC has been reported in several previous experimental studies.[4–11] Raman spectroscopy has been shown to be a valuable probe of SiC grown by a variety of techniques. The polytype dependence of the one-phonon Raman spectra of SiC, first noted by Choyke and collaborators,[4] has been shown to be of great significance.

Klein *et al.* established a theory of plasmon-phonon coupling in semiconductors which successfully predicted Raman line shapes for *n*-type nitrogen-doped 6H–SiC.[5] Furthermore, Klein and Colwell were the first to observe electronic Raman scattering from nitrogen-doped 6H–SiC at low temperature.[6] Following Ref. 6 there have been experimental studies of electronic Raman scattering from nitrogen donor levels in other SiC polytypes.[8,10] In contrast to 6H–SiC, the electronic Raman scattering in 4H–SiC is quite weak and quality experimental data is scarce.[10] It is important to note that these Raman studies used green or blue laser excitation. Under these conditions, electronic Raman scattering in nitrogen-doped silicon carbide is only clearly observed at low temperatures. It is generally accepted that nitrogen occupies carbon sites[12] in the SiC. In 4H–SiC, there are two inequivalent sites, one hexagonal and one quasicubic; for 6H–SiC, there are three sites, two quasicubic and one hexagonal.[10]

In this article, we present Raman scattering data from both 4H– and 6H–SiC which demonstrate that electronic Raman scattering from nitrogen defect levels can be resonantly enhanced with red or near-IR laser excitation at room temperature. The resonantly enhanced electronic Raman scattering is found to be polytype dependent. We also present similar data taken at low temperature that shows this effect with sharper, more intense peaks. In 4H–SiC, the resonantly enhanced peaks are seen to shift with doping concentration. We note that IR Raman scattering was found to be a valuable tool for the characterization of diamond films.[13]

EXPERIMENT

The Raman spectra were recorded using confocal Raman microscopy. A Dilor LabRam system and a Renishaw Series 1000 Raman microscope were both used. All micro-Raman data were collected at room temperature. Micro-Raman spectra were obtained with laser excitation at 785 nm (1.58 eV) and 633 nm (1.96 eV), which was compared with data taken at 514 nm (2.41 eV) with both a Raman microscope and a bulk Raman spectrometer. The bulk Raman spectrometer was also used to collect data using 568 nm (2.18 eV) and 647 nm (1.92 eV) laser excitation, and to take low temperature data using a crystal cooled with liquid nitrogen. This system has been previously described and used to examine SiC wafers.[11] The spectral resolution is approximately 1 cm^{-1} for the micro-Raman spectra. The experiments were all done in a

---

[a)] Author to whom correspondence should be addressed; electronic mail: fhlong@rutchem.rutgers.edu

0021-8979/99/86(4)/2073/5/$15.00

TABLE I. Peaks observed at room temperature assigned to nitrogen doping.

Polytype	Peak frequency (cm^{-1})	Label in figures
4H–SiC	400	N_a
	530	N_b
	570	N_c
6H–SiC	380	N_d
	430	N_e
	510	N_f
	638	N_g

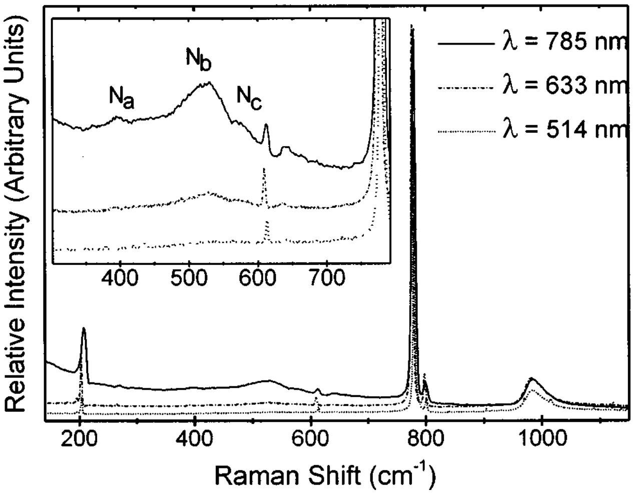

FIG. 1. Raman spectra from a single *n*-type 4H–SiC sample taken at room temperature with different laser excitation wavelengths: 514 nm (2.41 eV), 633 nm (1.98 eV), and 785 nm (1.58 eV). Note the clear appearance of several additional peaks, shown enlarged in the inset, labeled N_a, N_b, and N_c, as the laser wavelength is tuned to the near IR. We attribute these peaks to electronic Raman scattering from the nitrogen defect levels. The spectra are normalized to the peak at 777 cm^{-1}.

backscattering geometry with the light collected along or close to the *c* axis of the SiC. Confocal Raman spectra taken 5–10 μm below the surface of the SiC wafer yielded results very similar to the surface of the SiC; therefore, the effects we have observed are not surface specific. We have also observed similar effects in the micro-Raman spectra of epilayers of both 4H– and 6H–SiC at room temperature. The Raman spectra at different doping concentrations were normalized to the principal SiC Raman mode, which was not altered by doping.

The silicon carbide samples used were primarily wafers 1–2 in. in diameter and came from multiple sources. The results reported here are independent of sample origin. We studied a selection of *n*-type SiC samples with different doping ranging from nominally undoped (semi-insulating) to $7.1\times 10^{18}\,\mathrm{cm}^{-3}$.

RESULTS AND DISCUSSION

The major peaks in the Raman spectrum from 4H– or 6H–SiC remained the same between excitation at 514 nm and excitation at 785 nm, and have been identified in previous studies.[4–11] In 4H–SiC, the peak at 204 cm^{-1} is an E_2 planar or transverse acoustic mode, 610 cm^{-1} is A_1 axial or longitudinal acoustic, 777 cm^{-1} is E_2 planar optical, 797 cm^{-1} E_1, and 967 cm^{-1} is A_1 longitudinal optical. Analogous wavelength dependence was also observed for 6H–SiC. The primary peaks in 6H–SiC are an E_2 planar acoustic mode at 150 cm^{-1}, two planar or transverse optical modes of E_2 symmetry at 768 and 788 cm^{-1}, and an A_1 longitudinal optical phonon at 966 cm^{-1}. The mode at 796 cm^{-1} is a planar optical mode of E_1 symmetry. Further details can be found elsewhere.[11] We also note that some of these peaks exhibit Fano resonances under appropriate doping and laser excitation conditions.[6] The Raman peaks associated with nitrogen doping observed in 4H– and 6H–SiC are listed in Table I.

Figure 1 shows room-temperature Raman spectra of a single nitrogen-doped 4H–SiC wafer ($n=5.5\times 10^{18}\,\mathrm{cm}^{-3}$) which were taken at different laser excitation wavelengths: 514 nm (2.41 eV), 633 nm (1.98 eV), and 785 nm (1.58 eV). There is a very significant change in the Raman spectra upon changing the laser wavelength. When the laser excitation is in the red or near IR, clear resonant enhancements are observed for peaks at approximately 400, 530, and 570 cm^{-1}, enlarged and labeled N_a, N_b, and N_c in the inset. At 620 cm^{-1}, a Fano resonance is observed. We note that we have not found any changes in the major peaks of the spectrum. The intensity and Raman shift of these peaks is unaffected by the change in excitation to red light. The A_1(LO) mode behaves in the same manner as we have previously observed.[11] This contrasts with our preliminary studies using UV excitation which indicate that the signal from the A_1(LO) mode is significantly resonantly enhanced at those wavelengths.[14]

The strongest peak at 530 cm^{-1} (N_b) is broad and asymmetric; this asymmetry is possibly due to another peak near 500 cm^{-1}. The peaks at 530 and 570 cm^{-1} are consistent with previous measurements of *n*-type 4H–SiC at low temperature.[10] At low temperatures, a sharp peak at 57 cm^{-1} has also been measured.[10] The three high frequency peaks and the low frequency mode at 57 cm^{-1} make for a total of four peaks that can be attributed to nitrogen donors in 4H–SiC. This is more than the number of inequivalent sites, two, for 4H–SiC.

Figure 2 shows Raman spectra for *n*-type 4H–SiC at different doping concentrations, taken at room temperature with 785 nm (1.58 eV) excitation. As the *n*-type nitrogen doping concentration increases from semi-insulating to $7.1\times 10^{18}\,\mathrm{cm}^{-3}$, we clearly see an increase in the intensity of the peaks at approximately 400, 530, and 570 cm^{-1}. The absence of peaks N_a, N_b, and N_c in the semi-insulating sample demonstrates that these peaks are associated with nitrogen doping. In previous work,[11,15] we have drawn attention to a pedestal in the Raman spectrum beginning at around 500 cm^{-1}, which we attributed to a possible second-order scattering. This is also visible in the spectrum of the semi-insulating sample at 785 nm (1.58 eV), which shows further that the pedestal is unlikely to be due to nitrogen doping, and moreover is not a probable cause of the resonant effect that we report here. Careful inspection of the peak (N_b) near 530 cm^{-1} determines that the absolute peak position shifts to

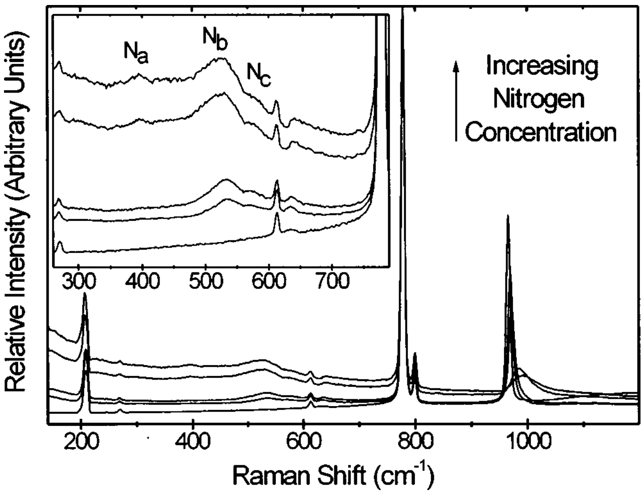

FIG. 2. Raman spectra for 4H–SiC taken at room temperature at 785 nm (1.58 eV) for different *n*-type doping concentrations. The peaks under discussion, N_a, N_b, and N_c, shown enlarged in the inset, are clearly not observed in the semi-insulating sample. The spectra are organized in order of doping concentration, with the highest at the top and the lowest at the bottom: 7.1×10^{18}, 5.5×10^{18}, 2.6×10^{18}, $2.1\times10^{18}\,\text{cm}^{-3}$, and semi-insulating. The spectra are normalized to the peak at 777 cm^{-1}.

smaller values of Raman shift as the nitrogen concentration is increased. This is illustrated clearly by Fig. 3, which shows the position of peak N_b at different doping concentrations. The open diamonds show the peak positions for the data shown in Fig. 2 and the solid squares show data taken from low-temperature Raman spectra taken with 647 nm (1.92 eV) laser excitation.

Figure 4 shows the Raman spectrum for a *n*-type nitrogen-doped ($2.1\times10^{18}\,\text{cm}^{-3}$) 6H–SiC sample taken at room temperature with 785 nm (1.58 eV) laser excitation. At least four additional peaks can be observed, which are labeled in the insert as N_d, N_e, N_f, and N_g. These peaks are not clearly visible in 6H–SiC at room temperature with 514 nm (2.41 eV) excitation (data not shown).[11] In fact, using 514 nm excitation the electronic Raman scattering peak at 510 cm^{-1} is masked by the weakly scattering 6H–SiC phonons at 505 and 513 cm^{-1}.[11]

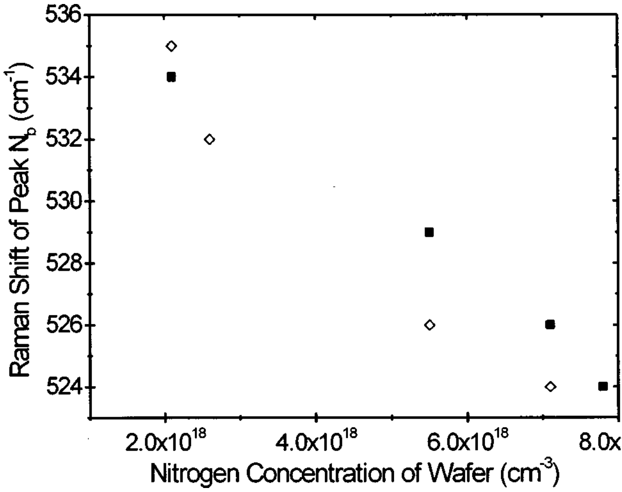

FIG. 3. Peak N_b Raman shift vs nominal doping concentration in 4H–SiC wafers. The open diamonds show the positions for the data in Fig. 2. The filled squares show data taken at low temperature using 647 nm (1.92 eV) laser excitation. A shift of 11 cm^{-1} is clearly seen over the concentration range studied.

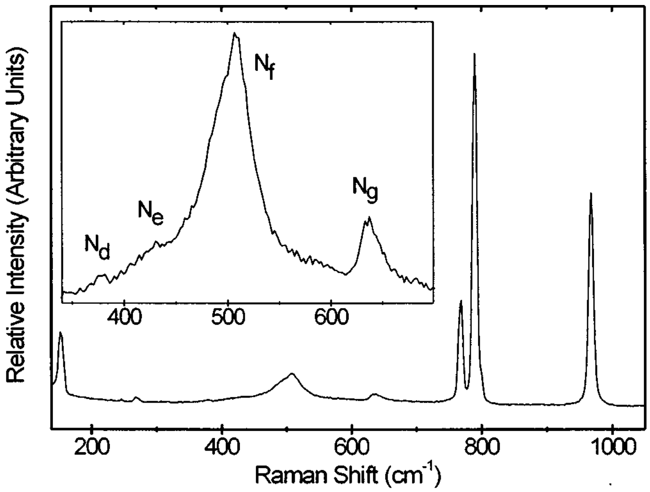

FIG. 4. Raman spectrum from 6H–SiC with *n*-type doping concentration of $2.1\times10^{18}\,\text{cm}^{-3}$, taken at room temperature with excitation at 785 nm (1.58 eV). Inset is an enlargement of the region between 350 and 700 cm^{-1}. Note the appearance of peaks attributable to nitrogen labeled N_d, N_e, N_f, and N_g.

In Figs. 5(a) and 5(b), we present low-temperature Raman spectra of 6H–SiC grown by two different methods. The spectra were taken using 647 nm laser excitation from samples held in a cryostat cooled with liquid nitrogen, and are normalized to the most intense peak at 788 cm^{-1}. It can clearly be seen that the resonant peaks sharpen up considerably at low temperature. We note that these sharper peaks are also visible when 514 nm excitation is used, as noted first by Klein and Colwell.[6] It is clear from Fig. 5(a) that the resonant spectrum of the platelet sample, grown by the Lely method, is more intense than that of the wafer sample, grown by state of the art methods. However, this difference in intensity is confined to these peaks. The other peaks in the spectrum [the A_1(LO) at around 965 cm^{-1} and E_2(PO) at around 768 cm^{-1}] are of comparable intensity in both spectra. Figure 5(b), which shows an enlargement of the region between 350 and 700 cm^{-1}, also shows that there is additional structure visible in the spectrum of the Lely grown platelet. Additional peaks are observed at about 377, 404, 427, 557, and 581 cm^{-1}. These peaks may be due to local vibrational modes of the nitrogen atom. This significant difference in the Raman spectra for samples with different growth methods may be due to a variety of factors. The mechanism by which the sample is grown and dopant is incorporated into the sample lattice obviously has a large influence on the properties of the sample. Further investigation of the reasons for these differences are ongoing in our laboratory.

Figure 6 compares Raman spectra with 647 nm (1.92 eV) excitation for two 4H–SiC samples at low temperature and room temperature. This illustrates the differences between the Raman spectra at different doping levels and temperatures. The semi-insulating sample shows no trace of resonant peaks at either temperature. It is also evident that

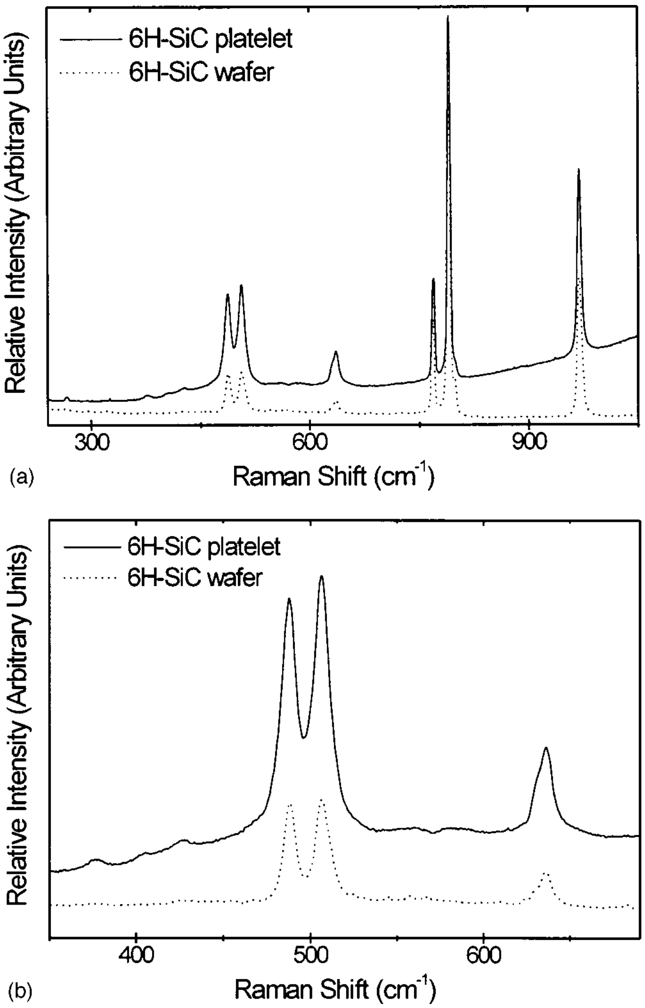

FIG. 5. (a) Raman spectrum of a 6H–SiC platelet grown by the Lely process compared with the Raman spectrum of a 6H–SiC wafer. (b) Same data as (a), but with an expanded scale which shows clearly the extra structure in the spectrum of the platelet that is not visible in the wafer spectrum.

the resonant peaks in the *n*-type doped sample are more intense at low temperature.

We have also observed that, for comparable nitrogen concentrations, it appears as if the electronic Raman scattering from nitrogen donor levels in 6H–SiC is much stronger than the 4H–SiC polytype. We demonstrate this in Fig. 7, which shows spectra of a sample of each polytype, normalized to their highest peaks. It is clear that the resonant peaks are much more intense in the 6H–SiC sample than the 4H–SiC sample. We have already shown that the intensity of the resonant peaks increases with doping level. We note that the 4H–SiC sample ($n = 5.5 \times 10^{18}\,\mathrm{cm}^{-3}$) actually has a higher concentration of *n*-type doping than the 6H–SiC ($n = 1.7 \times 10^{18}\,\mathrm{cm}^{-3}$), so the increased intensity in the 6H–SiC sample is not merely due to a doping effect. The peak at about 200 cm^{-1} in the 4H–SiC is a clear example of a Fano resonance, an asymmetry and distortion caused by overlap and interference between a broad electronic state and a discrete phonon state.[10] We note that the interference appears to increase as the laser excitation wavelength is tuned from the green to the near-IR, which suggests that the scattering from the electronic continuum is enhanced.

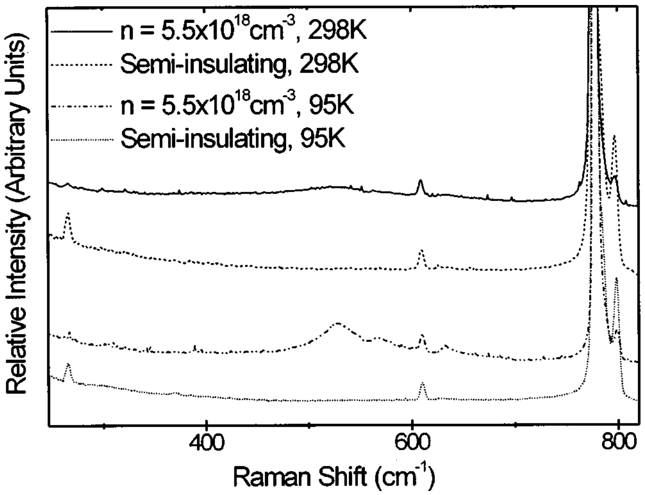

FIG. 6. Raman spectra of 4H–SiC wafers using laser excitation at 647 nm (1.92 eV). Low temperature data are contrasted with room temperature data for a moderately high doping concentration *n*-type wafer and a semi-insulating wafer. The semi-insulating sample shows no peaks in the region of interest. There is clearly a resonant peak in both spectra of the *n*-type wafer, which is enhanced at low temperatures.

The peaks observed in out Raman experiments are quite consistent with the values for electronic Raman scattering in *n*-type 6H–SiC established by Klein.[6] The peak observed by Klein at 113 cm^{-1} in *n*-type 6H–SiC appears in our data as a tail in the Raman spectrum, as shown in Fig. 4. Fano interference effects are observed in the peak at approximately 150 cm^{-1} due to these tails, again similar to effects were observed by Klein.[6] The Raman peaks at 486, 505, 635, and 642 cm^{-1} measured by Klein[6] and Gorban[8] at low temperature are quite consistent with the asymmetric peaks we observe in 6H–SiC around 510 and 638 cm^{-1} at room temperature.[6] As pointed out by Gorban *et al.* the number of electronic Raman peaks is not equal to the number of inequivalent carbon sites for 6H–SiC.[8]

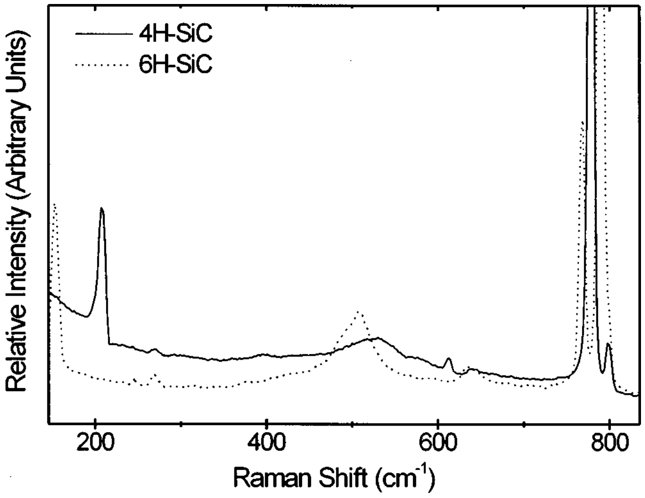

FIG. 7. Comparison of Raman spectra of 4H–SiC and 6H–SiC taken at room temperature using 647 nm (1.92 eV) laser excitation. The spectra are normalized by their most intense peaks. The resonance effect is clearly larger in the 6H–SiC sample, even though the 4H–SiC sample has a higher doping concentration.

Nitrogen-doped 4H– and 6H–SiC both have a greenish metallic color. In contrast, semi-insulating SiC is clear. The color is more intense in the heavily doped samples. The green color coincides with a broad electronic absorption in the near IR.[16,17] Although this visible and near-IR absorption in SiC was noted in the 1950s and 60s, it has not been definitively characterized. This absorption band is the probable origin of the resonance enhancements observed in the electronic Raman scattering from the nitrogen doping levels. The near-IR absorption seen in nitrogen-doped SiC is most likely due to the formation of deep defects. It is reasonable to assume that nitrogen doping of SiC is not unrelated to the well-studied problem of nitrogen doping of diamond. Nitrogen forms a deep level in diamond associated with lattice relaxation and an observed UV absorption inside the gap.[18]

The electronic spectrum of donors in SiC is of fundamental importance. In addition to electronic Raman scattering, Fourier-transform infrared measurements have also been made of the electronic energy levels of nitrogen donors in SiC.[19–21] The IR and electronic Raman transitions obey different selection rules and are therefore complementary measurements. Previous workers have identified the low frequency electronic Raman scattering peak as due to valley-orbit splitting of the electronic ground state, because of the anisotropic SiC band structure.[6,8] As noted earlier, and by other workers, the electronic spectrum of donors in SiC is complicated by the existence of inequivalent sites for both 6H– and 4H–SiC. It is also possible that some of the Raman peaks observed are nitrogen local modes, this will be the subject of further investigation.

SUMMARY

In summary, we have observed electronic Raman scattering from nitrogen donor levels in both 4H– and 6H–SiC. We have found that the electronic Raman scattering is enhanced with red or near-IR laser excitation. This resonance is due to the near-IR absorption, typical of nitrogen-doped SiC, which has been attributed to deep defects in the material. Future work will employ electronic Raman scattering to investigate the defect chemistry of nitrogen in silicon carbide.

ACKNOWLEDGMENTS

One of the authors (F.H.L.) would like to thank the Rutgers Research Council for their financial support. The work at EMCORE was funded by an SBIR Grant No. N00014-98-N-0050 monitored by Dr. Colin Wood of the Office of Naval Research. For assistance with Raman microscopy, the authors would like to thank Dr. Fran Adar and Robert Garton of Instruments SA and Dr. Mark Pavlosky of Renishaw Corporation.

[1] R. P. Devaty and W. J. Choyke, Phys. Status Solidi A **162**, 5 (1997).

[2] R. C. Glass, D. Henshall, V. F. Tsvetkov, and C. H. Carter, Mater. Res. Bull. **22**, 30 (1997).

[3] D. Hoffman, R. Eckstein, M. Kolbl, Y. Makarov, S. G. Muller, and E. Schmitt, J. Cryst. Growth **174**, 669 (1997).

[4] D. W. Feldman, J. H. Parker, Jr., W. J. Choyke, and L. Patrick, Phys. Rev. **173**, 787 (1968); **170**, 698 (1968).

[5] M. V. Klein, B. N. Ganguly, and P. J. Colwell, Phys. Rev. B **6**, 2380 (1972).

[6] P. J. Colwell and M. V. Klein, Phys. Rev. B **6**, 498 (1972).

[7] D. Olego, M. Cardona, and P. Vogl, Phys. Rev. B **25**, 3878 (1982).

[8] I. S. Gorban, V. A. Gubanov, V. D. Kulakovskii, A. S. Skirda, and B. N. Shepel', Sov. Phys. Semicond. **30**, 928 (1988).

[9] J. Liu and Y. K. Vohra, Phys. Rev. Lett. **72**, 4105 (1994).

[10] S. Nakashima and H. Harima, Phys. Status Solidi A **162**, 39 (1997).

[11] J. C. Burton, L. Sun, M. Pophristic, S. Lukacs, F. H. Long, Z. C. Feng, and I. T. Ferguson, J. Appl. Phys. **84**, 6268 (1998).

[12] H. H. Woodbury and G. W. Ludwig, Phys. Rev. **124**, 1083 (1961).

[13] W. Wörner, J. Wagner, W. Müller-Sebert, C. Wild, and P. Koidl, Appl. Phys. Lett. **68**, 1482 (1996).

[14] J. C. Burton and F. H. Long (unpublished results).

[15] J. C. Burton, L. Sun, F. H. Long, Z. C. Feng, and I. T. Ferguson, Phys. Rev. B **59**, 7282 (1999).

[16] G. B. Dubrovskii and E. I. Radovanova, Sov. Phys. Solid State **11**, 545 (1969).

[17] E. Biedermann, Solid State Commun. **3**, 343 (1965).

[18] P. R. Briddon and R. Jones, Physica B **185**, 179 (1993).

[19] W. Suttrop, G. Pensl, W. J. Choyke, R. Stein, and S. Leibenzender, J. Appl. Phys. **72**, 3708 (1992).

[20] W. Götz, A. Schöner, G. Pensl, W. Suttrop, W. J. Choyke, R. Stein, and S. Leibenzender, J. Appl. Phys. **73**, 3332 (1993).

[21] W. J. Moore, P. J. Lin-Chung, J. A. Freitas, Jr., Y. M. Altaiskii, V. L. Zuev, and L. Ivanova, Phys. Rev. B **48**, 12289 (1993).